Available online at www.sciencedirect.com

SciVerse ScienceDirect

Ceramics International 38 (2012) 6635–6641

CERAMICS INTERNATIONAL

www.elsevier.com/locate/ceramint

Silica coated ferrite nanoparticles: Influence of citrate functionalization procedure on final particle morphology

Bojana Mojić[a,*], Konstantinos P. Giannakopoulos[b], Željka Cvejić[c], Vladimir V. Srdić[a]

[a]*Department of Materials Engineering, Faculty of Technology, University of Novi Sad, Novi Sad, Serbia*
[b]*Institute of Microelectronics, National Centre for Scientific Research "Demokritos", Athens, Greece*
[c]*Department of Physics, Faculty of Natural Sciences, University of Novi Sad, Novi Sad, Serbia*

Received 8 March 2012; received in revised form 23 April 2012; accepted 16 May 2012
Available online 23 May 2012

Abstract

In this paper, magnetic nanoparticles (Fe_3O_4 and $NiFe_2O_4$) were coated with a biocompatible silica shell via hydrolysis and condensation of tetraethyl orthosilicate (TEOS) by the Stöber process. Magnetic nanoparticles, prepared by chemical co-precipitation from iron and nickel salts, were functionalized with citric acid, in order to provide their deagglomeration and to enable their coating with silica. The parameters of the functionalization procedure were varied (concentration–pH and type of treatment), in order to examine if and how this particular step of preparation affects the final morphology of the core-shell particles. Transmission electron microscopy, zeta potential and particle size measurements revealed that the morphology and the size of obtained core shell particles depend significantly on the core particle size, and thus on the parameters of the functionalization step.

Keywords: A. Powders: chemical preparation; B. Nanocomposites; D. Ferrites

1. Introduction

Oxide magnetic nanomaterials, and especially ferrites, are nowadays intensively studied because of their numerous applications, such as those in high density storage media, high frequency devices, magnetically assisted drug delivery, immobilization of proteins and enzymes and waste-water treatment [1–4]. However, it is often necessary to coat the particles with another material or embed them in a non-magnetic matrix, in order to prevent their agglomeration and sedimentation, or to make them biocompatible and suitable for specific applications [5]. In recent years, silica has been widely used as a coating material. Its biocompatibility, stability against degradation, and easy surface modification due to the abundant silanol groups, is making silica microspheres of particular interest for use in biomedicine and bioengineering. Furthermore, a silica shell could screen magnetic dipole interactions between magnetic nanoparticles, and in that way facilitate their dispersion in liquid media [6]. Therefore, various methods for obtaining a silica shell on the surface of magnetic nanoparticles have been developed, and a sol–gel method based on the well-known Stöber process [7] has been widely used [5,8–11], mostly for its low-cost and mild reaction conditions. Recently, systematic studies on the coating of magnetite particles with silica through a sol–gel process have been reported by Deng et al. [5] and Haw et al. [12], emphasizing mostly the influence of precursor ratios, precursors and the surfactant type on the morphology and final characteristics of the obtained structures. In both studies, a treatment of magnetite particles with citric acid was performed prior to their coating with silica. In general, the modification of ferrite nanoparticles with biocompatible citric acid, as a method for overcoming particle agglomeration, has been widely performed and studied [13–15]. However, the influence of the modification protocol, morphology and size of the citrate-modified nanoparticles, on the final morphology of silica coated core-shell particles, did not

*Correspondence to: Department of Materials Engineering, Faculty of Technology, University of Novi Sad, Bulevar Cara Lazara 1, 21000 Novi Sad, Serbia. Tel.: +381 214 853665; fax: +381 214 50413.
E-mail address: bojanamojic@gmail.com (B. Mojić).

0272-8842/$36.00
http://dx.doi.org/10.1016/j.ceramint.2012.05.050

receive much attention. In this work, a possible approach for coating magnetic (nickel ferrite and magnetite) nanoparticles with silica is reported, whereby special attention has been paid to the relation of the citrate-modification procedure and the final morphology of the core shell particles.

2. Experimental

Silica coated magnetic nanoparticles were prepared by a three-step procedure. Firstly, magnetic nanoparticles of magnetite (Fe_3O_4) and nickel ferrite ($NiFe_2O_4$) were prepared by the co-precipitation method. In the second step, water washed magnetic nanoparticles were treated with citric acid (CA) in order to prevent their agglomeration and finally, silica coating was formed on their surface via hydrolysis and condensation of tetraethyl orthosilicate (TEOS), by the Stöber process.

2.1. Materials

Analytical-grade tetraethyl orthosilicate (TEOS, ≤ 98 wt%), ethyl alcohol (>99.9 wt%), ammonia solution (NH_3, 25 wt%), sodium hydroxide pellets (NaOH, assay ≥ 97 wt%), and ferrous sulfate $FeSO_4 \times 7H_2O$ (assay ≥ 99 wt%) were purchased from Merck, Germany. Ferric nitrate $Fe(NO_3)_3 \times 9H_2O$ (assay ≥ 99 wt%), nickel nitrate $Ni(NO_3)_2 \times 6H_2O$ (assay ≥ 99 wt%) and anhydrous citric acid, CA (99 wt%) were purchased from Sigma Aldrich, Germany. Chemicals were used as received, without further purification. Deionized water was used throughout the experiments.

2.2. Preparation of magnetic nanoparticles

Magnetic (Fe_3O_4 and $NiFe_2O_4$) nanoparticles, MNP, were prepared by low temperature chemical co-precipitation, using aqueous solutions of iron and nickel salts. The stoichiometric amounts of $Fe(NO_3)_3 \times 9H_2O$ and $FeSO_4 \times 7H_2O$ or $Ni(NO_3)_2 \times 6H_2O$ were dissolved in deionized water with the concentration of 0.15 mol/L; sodium hydroxide solution was added dropwise, until pH reached ~ 12. The reaction was kept under constant stirring at 80 °C for 1 h. Precipitated ferrite nanopowders were washed with deionized water and one aliquot was separated for further examination. The obtained magnetite and nickel ferrite powders were denoted as M_0 and NF_0, respectively.

2.3. Citrate modification of magnetic nanoparticles

Washed magnetic nanoparticles (MNP) were dispersed in deionized water in the concentration of 1.5 g/L. The dispersions were treated with 1 M CA in different amounts and consequently at different pH values and further stirred or ultrasonically agitated for 30 min, in order to obtain stabilization of MNP. All experiments were performed at room temperature. Parameters of modification were varied in order to examine the impact of the modification procedure on the morphology of the final product, silica coated magnetic nanoparticles. Sample notation and processing parameters are outlined in Table 1.

Table 1
Sample denotation.

Sample code	Material	CA [mmol/g]	pH	Treatment
NF_0	$NiFe_2O_4$	–	–	–
M_0	Fe_3O_4	–	–	–
NF_1	$NiFe_2O_4$	7	3	Stirring
NF_2	$NiFe_2O_4$	3.5	5	Stirring
NF_3	$NiFe_2O_4$	3.5	5	Ultrasound
M_1	Fe_3O_4	3.5	5	Stirring

2.4. Coating of magnetic nanoclusters with silica

Dispersions of citrate modified nanoparticles were used as core particles on which silica coating was obtained by the Stöber process [7]. Aqueous magnetic fluids (noted as NF_1, M_1, NF_2, NF_3), adjusted to the concentration of 1 g/L were added to an ethanol and ammonia aqueous mixture and were dispersed ultrasonically. Finally, TEOS was added dropwise to the dispersion under constant stirring. The amount of 1 mmol of TEOS was added to the dispersion containing 10 ml of magnetic fluid, 40 ml of ethanol and 1.5 ml of ammonia. The reaction was carried out under constant stirring at room temperature, for 6 h. The light orange precipitated powder was centrifuged and washed with distilled water until the effluent was free of NH_4^+ groups, and was finally dried at 120 °C for 1 day. The samples of magnetic nanoparticles coated with silica were denoted as SNF_1, SM_1, SNF_2, SNF_3, according to the name of the specific magnetic fluid used for the core particles.

2.5. Powder characterization

The particle size distribution (by intensity and number) of citrate modified magnetic nanoparticles and silica coated nanoparticles was measured by dynamic light scattering, DLS (Zetasizer Nano ZS, Malvern Instruments, Malvern, United Kingdom). Refractive indexes of 2.42 and 2.3 were used for Fe_3O_4 and $NiFe_2O_4$ particles, respectively. All measurements were performed at pH ~ 7. Zeta potential was determined by the same instrument (Zetasizer Nano ZS with MPT-2 Autotitrator Malvern Instruments, Malvern, United Kingdom), using the M3-PALS method, i.e. the combination of laser doppler velocimetry and phase analysis light scattering. The morphology, the shape and the crystallinity of the silica-coated nanoparticles were analyzed using a transmission electron microscope, TEM (Philips CM 20, Eindhoven, Netherlands) operating at 200 kV, equipped with an energy-dispersive X-ray spectroscopy system (EDS). TEM samples were

prepared by drying one drop of ultrasonically dispersed particles on a carbon film supported by a Cu-grid. X-ray diffraction (XRD) of the powders was performed using a PANalytical X-ray diffractometer (X'Pert PRO) with a Ni-filter and Cu$K\alpha$ radiation, operating at 40 mV and 40 mA. The measurements were obtained with a step size of 0.033° and speed of 0.005°/s. The crystallite size of ferrite nanopowders was estimated using the Scherrer equation ($d=0.9\lambda/(\beta\cos\theta)$ [16], λ is the wavelength of the X-rays, θ is the scattering angle of the Bragg reflections, β is the full width at half maximum). Fourier-transform infrared spectroscopy measurements were performed using a Nicolet-Nexsus 670 FT-IR.

3. Results and discussion

3.1. Characterization of ferrite nanopowders

The one-step synthesis by co-precipitation at pH∼12 and $T=80$ °C resulted in polycrystalline ferrite nanopowders. Thus, the XRD pattern of the magnetite M_0 powder has all the characteristic reflections of the cubic spinel phase (Fig. 1). The average crystallite size, calculated from XRD peak broadening using Scherrer's formula is 17.5 nm. On the other hand, the diffractogram of the as-synthesized NF_0 ($NiFe_2O_4$) powder (Fig. 1) confirms that in this case either significantly smaller crystallites of a size ∼3 nm or less ordered structures were formed. The as-synthesized black (M_0) and dark-red (NF_0) nanopowders exhibited magnetic behavior in the presence of 0.3 T permanent magnet.

The ferrite nanoparticles, prepared by co-precipitation, are hardly agglomerated due to their large surface to volume ratio and high surface energies [17]. To overcome the agglomeration and enable their coating with silica, citric acid (CA) has been used for stabilization and surface modification of the as-synthesized ferrite nanoparticles, since it has the advantage of biocompatibility and non-toxicity [18]. In order to examine the effect of citric acid functionalization step on the size of the nickel ferrite core and the morphology of the core shell particles, zeta potential measurements of nickel ferrite particles, before and after surface functionalization were conducted (Fig. 2). The isoelectric point of the non-modified $NiFe_2O_4$ (NF_0) is at pH∼7, which is in good agreement with previously reported values [19,20]. On the other hand, in the case of the modified nanoparticles, a shift of the zeta potential towards more negative values was observed, together with a negative particle charge in the whole pH range, indicating the adsorption of citric acid at the particle surfaces. Fourier-transform infrared, FTIR, spectra (Fig. 3) of the as-synthesized and functionalized $NiFe_2O_4$ (NF_0 and NF_1) show peaks at ∼590 cm^{-1} and ∼430 cm^{-1} characteristic of the Ni–O stretching modes in $NiFe_2O_4$. In addition, spectra of the citrate-functionalized sample NF_1 show two intense bands at ∼1600 cm^{-1} and ∼1400 cm^{-1}, corresponding respectively to the symmetric

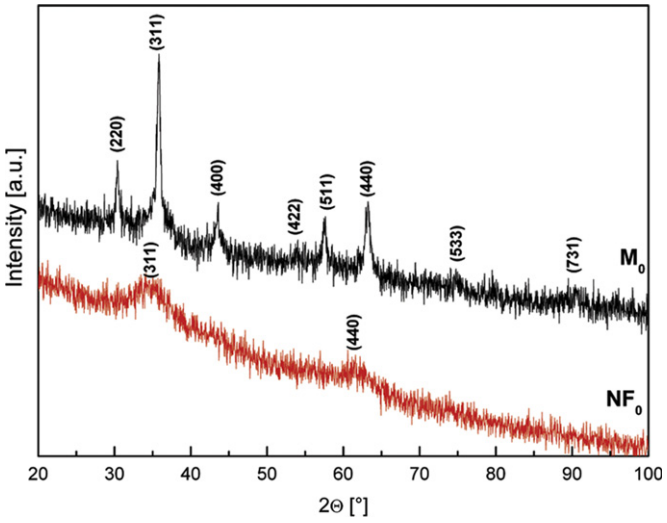

Fig. 1. XRD patterns of as-synthesized M_0 and NF_0 nanopowders.

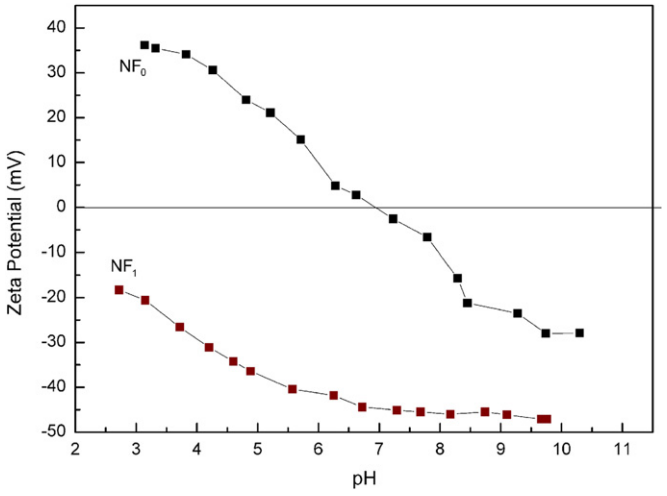

Fig. 2. Zeta potential of nickel ferrite nanoparticles as a function of pH, before (sample NF_0) and after (sample NF_1) the modification with citric acid.

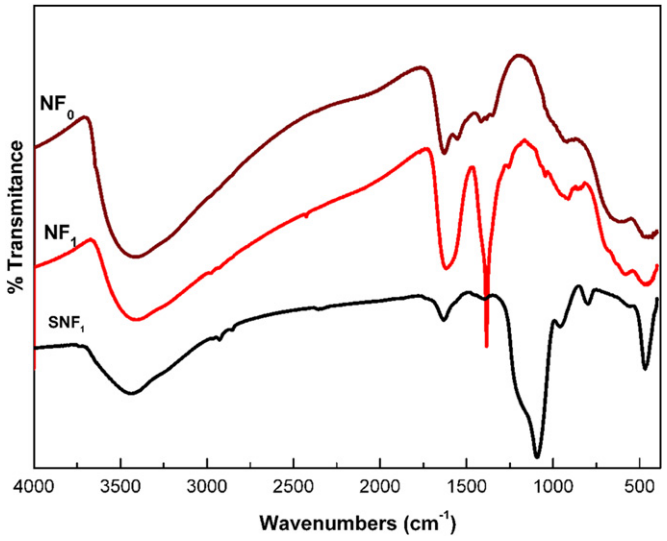

Fig. 3. FTIR spectra of NF_0, NF_1 and SNF_1 powders.

and asymmetric stretching of CO in the COOH group, confirming the binding of citric acid to the particle surface.

As proposed in a recent paper [21], citric acid may be adsorbed on the surface of the magnetite nanoparticles by co-ordinating via one or two of the carboxylate functionalities depending on the steric necessity and the curvature of the surface, leaving at least one carboxylic acid group exposed to the solvent, and thus making the surface charged. This can effectively prevent agglomeration of magnetic oxide nanoparticles, due to steric and electrostatic forces arising from the ionized layer of the citrate coating on the surface [15,21]. In our work, the visual appearance of magnetic fluid, after the addition of CA, had already indicated deagglomeration of the particles; the suspension became more transparent and no more sediment at the bottom of the glass vessel could be observed.

3.2. Characterization of core-shell particles

After subsequent coating of functionalized MNP, the light orange color of the precipitated powder indicated the successful adsorption of a silica shell. The structure of the $NiFe_2O_4$ particles stabilized with citric acid, and then coated with silica (sample SNF_1), was investigated by Fourier-transform infrared spectroscopy, FTIR (Fig. 3). Similar to the two other spectra, spectra of this sample show two broad bands at $\sim$3430 cm^{-1} and $\sim$1620 cm^{-1}, associated with the stretching vibration of free or adsorbed water that still remained in the sample. Bands at $\sim$1095 cm^{-1}, and $\sim$800 cm^{-1} correspond to the stretching of Si–O–Si bond of silica, while the band at $\sim$955 cm^{-1} could be assigned to the Si–O–H stretching vibration and Fe–O–Si vibration and the band at $\sim$470 cm^{-1} to Si–O–Si or O–Si–O bending mode [12,13,21]. In the same sample, bands at 1624 cm^{-1} and 1400 cm^{-1} are probably pronounced due to increased symmetric and asymmetric stretching of COO^-. This spectrum, on the other hand, does not show the peaks characteristic for metal–oxide bonds of ferrite particles, even though a small knee at $\sim$590 cm^{-1} is visible. However, although the spectra of the core/shell sample clearly indicates the adsorption of silica coating on the surface of ferrite particles, in order to confirm the existence of the ferrite core and to investigate particle morphology, samples were further examined by transmission electron microscopy.

The as-synthesized SNF_1 particles are mostly spherical with a characteristic core-shell structure (Fig. 4a–c). Neither core-free silica spheres, nor silica-free ferrite nanoparticles can be noticed, indicating that the chosen ratio of $NiFe_2O_4$ and TEOS as well as selected synthesis conditions were suitable for shell formation. Although the average particle size from TEM micrographs (Fig. 4a) is found to be $\sim$85 nm, with the shell thickness of $\sim$20 nm, bimodal size distribution (Fig. 4b) and the presence of considerably larger particles of $\sim$250 nm with shell of $\sim$70 nm can be noticed (Fig. 4b and c). This can be related to the bi-modal size distribution of the $NiFe_2O_4$ particles used as a core, confirmed by DLS measurement (Fig. 5a). The bi-modal size distribution of the ferrite NF_1 powder is attributed to the relatively low surface charge of the core particles at pH$\sim$3 (Fig. 2), that is insufficient for good particle stabilization [22,23], and which is probably caused by the suppressed dissociation of the carboxylic groups of CA adsorbed below pH$\sim$5.

In order to improve particle morphology, citrate functionalization of core particles was performed at higher pH ($\sim$5) providing higher surface charge and thus a more effective particle deagglomeration and consequently, a smaller particle size. Particle size measurements of the samples NF_2, NF_3 and M_1 confirmed a considerably smaller particle size (in comparison to the powder NF_1) caused by stabilization at pH$\sim$5, and at the same time revealed the influence of the type of particle treatment (ultrasound/stirring) (Fig. 5a). Using the Mie Theory, particle size distribution by intensity can be converted into the particle size distribution by number, in order to determine smaller differences in the particle size of core modified particles (Fig. 5b). The smallest average particle size ($\sim$15 nm) was measured for the sample treated ultrasonically (NF_3), what indicates the enhanced adsorption and higher uptake of citric acid by the particles subjected to ultrasonification, as previously reported by Zhang et al. [24]. However, since the concentration of citric acid added is sufficiently high, we assume that the smaller

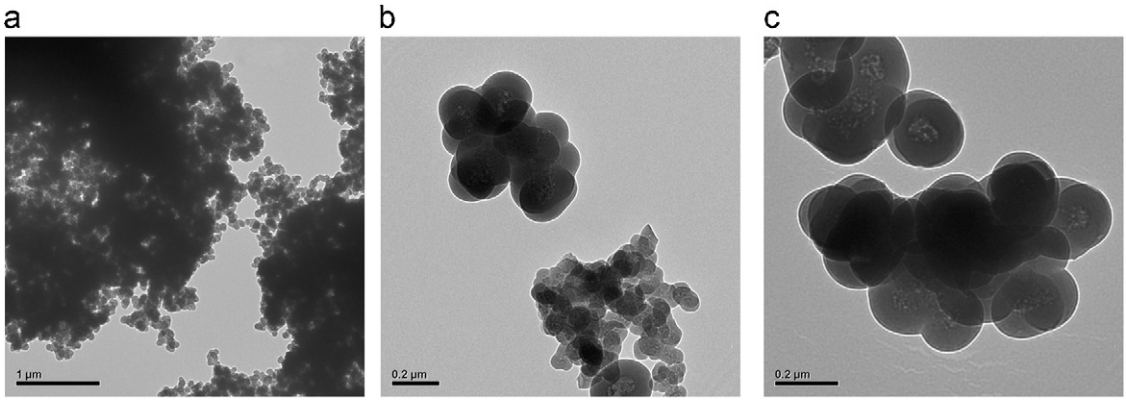

Fig. 4. TEM micrographs of the sample SNF_1.

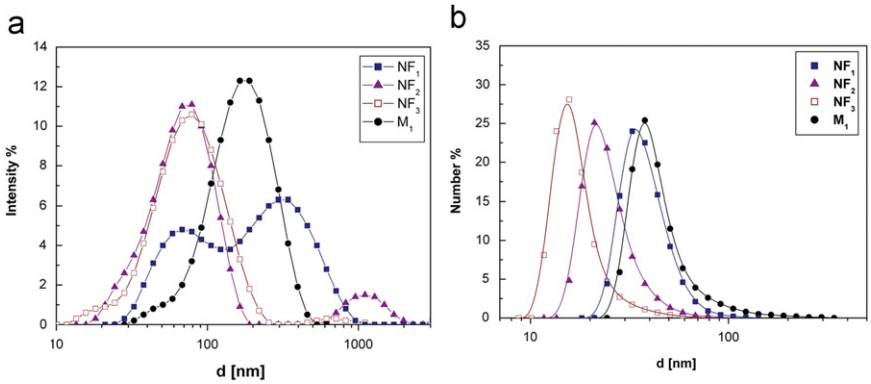

Fig. 5. Particle size distribution of citrate functionalized ferrite core particles by: (a) intensity and (b) number.

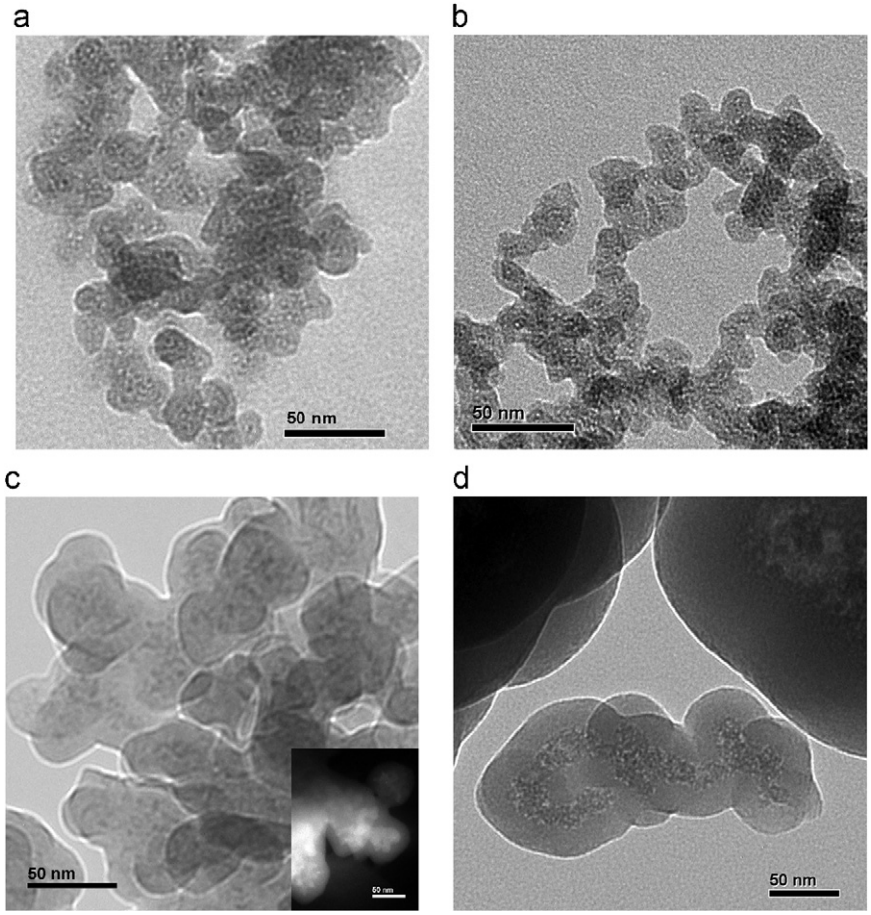

Fig. 6. TEM micrographs of samples: (a) SNF_2, (b) SNF_3, (c) SM_1, and (d) SNF_1.

particle size of the sample NF_3, compared to the sample NF_2 (~20 nm), was a result of deagglomeration which occurred under ultrasonic agitation, thus providing larger surface available for citrate adsorption, resulting in smaller nanoclusters of primary particles. The citrate functionalized magnetite (M_1), has shown larger average particle size than the sample of nickel ferrite treated in the same way (NF_2). This could be expected due to considerably larger crystallite size of precipitated powder M_0 comparing to the powder NF_0.

The increase of citric acid concentration was not found to be linked to the final particle size, which is explained by the fact that citric acid is adsorbed on the ferrite particle surface via one or two carboxylate groups even in its high excess, and therefore both the number of unbound groups and the overcharging of particles are limited [15].

TEM micrographs of silica coated samples SNF_2, SNF_3 and SM_1, presented in Fig. 6a–c, revealed considerably smaller particles than in the case of SNF_1 (Fig. 6d), with a

relatively large size distribution. Taking into consideration that the precursor ratio and the reaction parameters for the shell creation were identical for all the core-shell samples, it is obvious that the mentioned variations of morphology derive from the differences of the ferrite particles (clusters) used as cores. The SNF_2 and SNF_3 core-shell particles have similar morphology, with the average particle size of ~25 nm and ~20 nm, respectively (results obtained by image analysis) (Fig. 6a and b). Sample SM_1 showed similar morphology, but somewhat bigger size (~50 nm), clearly caused by bigger crystallite and thus particle size of magnetite core, as can be concluded from a dark field micrograph (Fig. 6c). Again depending on the effectiveness of the modification procedure, more or less agglomerated or even chain-like structures can be noticed throughout the samples, emphasizing the importance of the particle modification step in the procedure of the core-shell formation.

All XRD patterns of silica coated samples have the characteristic appearance of amorphous silica, with a diffusive peak at ~20°. However, discreet bumps in the place of potential strongest peaks (~36° and ~62°), characteristic for spinel ferrite phases, are visible in all samples (Fig. 7).

In order to confirm the composition of core-shell particles, EDS analysis was performed (Fig. 8) in the TEM with a Cu sample holder. EDS spectra clearly show the presence of all consisting elements (Si, O, Fe and Ni) which, in combination with XRD and FTIR results indicates the presence of $NiFe_2O_4$ and Fe_3O_4 particles coated with silica.

Characterization of the magnetic properties of the core-shell particles was not carried out during this work. However, the magnetic behavior of the particles and thus their suitability for certain in-vitro biomedical applications has been confirmed with the presence of 0.3 T permanent magnet, as can be seen in Fig. 9.

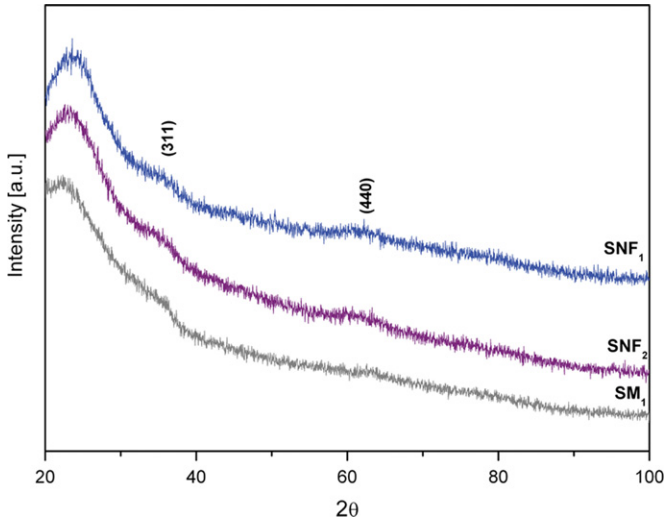

Fig. 7. XRD patterns of core shell samples.

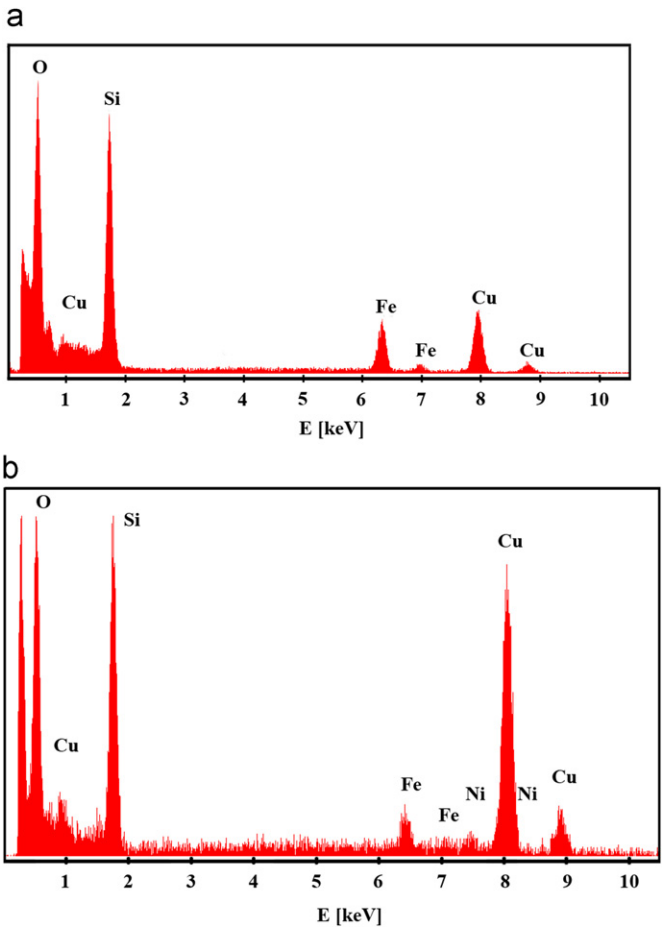

Fig. 8. EDS spectra of core shell particles: (a) SM_1 and (b) SNF_2.

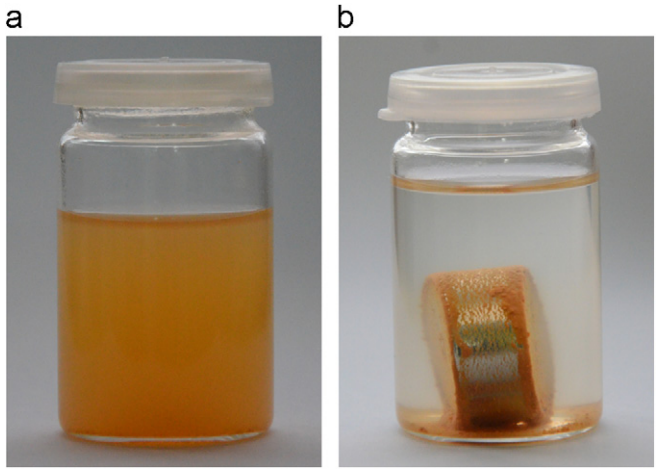

Fig. 9. Appearance of the core-shell particle dispersion in the (a) absence and (b) presence of permanent magnet (sample SNF_1).

4. Conclusion

By co-precipitation of magnetic particles ($NiFe_2O_4$ and Fe_3O_4) and by further hydrolysis and condensation of

TEOS on their surface, silica coated magnetic nanoparticles with a spherical morphology were synthesized. In the case of nickel ferrite core, clusters of magnetic nanoparticles modified with citric acid were prepared under different conditions and then coated with silica. It was found that a modification procedure (including pH/concentration and type of treatment) influences the final morphology of these core-shell particles and especially their size, morphology, agglomeration and shell thickness. Modification at lower pH ($\sim$3), resulted in larger nickel ferrite clusters and so larger core-shell particles were prepared, when compared to the ones prepared from the particles modified at pH$\sim$5. In the same way, modification by ultrasonification or by stirring, affected the size of the nickel ferrite clusters, and consequently, the size of core shell particles (after coating them with silica). The close relationship between core morphology and core shell morphology was clearly confirmed even within one sample; it was shown that bimodal size distribution of core particles has caused bimodal size distribution of final core shell particles. Even though the effect of citrate treatment on the morphology of core shell particles in the case of magnetite core was not examined, similar conclusions might be expected. All the core-shell particles exhibited magnetic behavior in the presence of a permanent magnet, confirming their suitability for certain in-situ biomedical applications.

Acknowledgment

The authors gratefully acknowledge the financial support provided by the Ministry of Science of the Republic of Serbia, Project no. III45021, and COST Project no. MP0904.

References

[1] D.S. Mathew, R.-S. Juang, An overview of the structure and magnetism of spinel ferrite nanoparticles and their synthesis in microemulsions, Chemical Engineering Journal 129 (1-3) (2007) 51–65.

[2] A. Chaudhuri, M. Mandal, K. Mandal, Preparation and study of $NiFe_2O_4/SiO_2$ core-shell nanocomposites, Journal of Alloys and Compounds 487 (1–2) (2009) 698–702.

[3] S. Singhal, J. Singh, S.K. Barthwal, K. Chandra, Preparation and characterization of nanosize nickel-substituted cobalt ferrites ($Co_{1-x}Ni_xFe_2O_4$), Journal of Solid State Chemistry 178 (10) (2005) 3183–3189.

[4] N. Insin, J.B. Tracy, H. Lee, J.P. Zimmer, R.M. Westervelt, M.G. Bawendi, Incorporation of iron oxide nanoparticles and quantum dots into silica microspheres, ACS Nano 2 (2) (2008) 197–202.

[5] Y.-H. Deng, C.-C. Wang, J.-H. Hu, W.-L. Yang, S.-K. Fu, Investigation of formation of silica-coated magnetite nanoparticles via sol–gel approach, Colloids and Surfaces A: Physicochemical and Engineering Aspects 262 (2005) 87–93.

[6] Y. Sun, L. Duan, Z. Guo, Y. DuanMu, M. Ma, L. Xu, Y. Zhang, N. Gu, An improved way to prepare superparamagnetic magnetite–silica core-shell nanoparticles for possible biological application, Journal of Magnetism and Magnetic Materials 285 (2005) 65–70.

[7] W. Stöber, A. Fink, E. Bohn, Controlled growth of mesoporous silica spheres in the micron size range, Journal of Colloid and Interface Science 26 (1) (1968) 62–69.

[8] Z. Lu, Y. Yin, B.T. Mayers, Y. Xia, Modyfying the surface properties of superparamagnetic iron oxide nanoparticles through a sol–gel approach, Nano Letters 2 (3) (2002) 183–186.

[9] S. Zhang, D. Dong, Y. Sui, Z. Liu, H. Wang, Z. Qian, W. Su, Preparation of core shell particles consisting of cobalt ferrite and silica by sol–gel process, Journal of Alloys and Compounds 415 (1–2) (2006) 257–260.

[10] J. Dong, Z. Xu, F. Wang, Engineering and characterization of mesoporous silica-coated magnetic particles for mercury removal from industrial effluents, Applied Surface Science 254 (11) (2008) 3522–3530.

[11] F. Mazaleyrat, M. Ammar, M. LoBue, J.-P. Bonnet, P. Audebert, G.-Y. Wang, Y. Champion, M. Hÿtch, E. Snoeck, Silica coated nanoparticles: synthesis, magnetic properties and spin structure, Journal of Alloys and Compounds 483 (1-2) (2009) 473–478.

[12] C.Y. Haw, C.H. Chia, S. Zakaria, F. Mohamed, S. Radiman, C.H. Teh, P.S. Khiew, W.S. Chiu, N.M. Huang, Morphological studies of randomized dispersion magnetite nanoclusters coated with silica, Ceramics International 37 (2) (2011) 451–464.

[13] P.C. Morais, R.L. Santos, A.C.M. Pimenta, R.B. Azevedo, E.C.D. Lima, Preparation and characterization of ultra-stabile biocompatibile magnetic fluids using citrate-coated cobalt ferrite nanoparticles, Thin Solid Films 515 (1) (2006) 266–270.

[14] M. Racuciu, Synthesis protocol influence on aquous magnetic fluid properties, Current Applied Physics 9 (5) (2009) 1062–1066.

[15] A. Hajdu, E. Illes, E. Tombacz, I. Borbath, Surface charging, polyanionic coating and colloid stability of magnetite nanoparticles, Colloids and Surfaces A: Physicochemical and Engineering Aspects 347 (1–3) (2009) 104–108.

[16] J.I. Langford, A.J.C. Wilson, Scherrer after sixty years: a survey and some new results in the determination of crystallite size, Journal of Applied Crystallography 11 (1978) 102–113.

[17] A.-H. Lu, E.L. Salabas, F. Schuth, Magnetic nanoparticles: synthesis, protection, functionalization, and application, Angewandte Chemie, International Edition 46 (8) (2007) 1222–1244.

[18] L.V. Thomas, U. Arun, S. Remya, P.D. Nair, A biodegradable and biocompatible PVA–citric acid polyester with potential applications as matrix for vascular tissue engineering, Journal of Materials Science: Materials in Medicine 20 (2009) S259–S269.

[19] R.C. Plaza, J. de Vicente, S. Gomez-Lopera, A.V. Delgado, Stability of dispersions of colloidal nickel ferrite spheres, Journal of Colloid and Interface Science 242 (2) (2001) 306–313.

[20] H. Yin, H.P. Too, G.M. Chow, The effects of particle size and surface coating on the cytotoxicity of nickel ferrite, Biomaterials 26 (29) (2005) 5818–5826.

[21] A. Goodarzi, Y. Sahoo, M.T. Swihart, P.N. Prasad, Aqueous ferrofluid of citric acid coated magnetite particles, Materials Research Society Symposium Proceedings 789 (6) (2004) 6.6.1–6.6.6.

[22] Zeta Potential of Colloids in Water and Waste Water, ASTM Standard D 4187-82, American Society for Testing and Materials, 1985.

[23] Y. Si, E.T. Samulski, Synthesis of water soluble graphene, Nano Letters 8 (6) (2008) 1679–1682.

[24] Y. Zhang, N. Kallay, E. Matijevic, Interactions of metal hydrous oxiders with chelating agents. hematite-oxalic acid and citric acid systems, Langmuir 1 (2) (1985) 201–206.